Plant Biotechnology Journal
Open Access

Plant Biotechnology Journal (2022) **20**, pp. 1856–1858 doi: 10.1111/pbi.13899

Brief Communication

The genome of *Eustoma grandiflorum* reveals the whole-genome triplication event contributing to ornamental traits in cultivated lisianthus

Yuwei Liang[1,†], Fan Li[2,†], Qiang Gao[1,†], Chunlian Jin[2], Liqing Dong[3], Qi Wang[1], Min Xu[1], Fuhui Sun[1], Bo Bi[1,4], Peng Zhao[3], Shenchong Li[2], Jiwei Ruan[2], Xiaofan Zhou[5,*], Liangsheng Zhang[1,6,*] and Jihua Wang[2,*]

[1]*Genomics and Genetic Engineering Laboratory of Ornamental Plants, College of Agriculture and Biotechnology, Zhejiang University, Hangzhou, China*
[2]*Floriculture Research Institute, Yunnan Academy of Agricultural Sciences, National Engineering Research Center for Ornamental Horticulture, Key Laboratory for Flower Breeding of Yunnan Province, Kunming, China*
[3]*School of Agriculture, Yunnan University, Kunming, China*
[4]*ZJU-Hangzhou Global Scientific and Technological Innovation Center, Hangzhou, China*
[5]*Guangdong Laboratory for Lingnan Modern Agriculture, Guangdong Province Key Laboratory of Microbial Signals and Disease Control, Integrative Microbiology Research Center, South China Agricultural University, Guangzhou, China*
[6]*Hainan Institute of Zhejiang University, Sanya, China*

Received 11 May 2022;
revised 5 July 2022;
accepted 22 July 2022.
**Correspondence* emails xiaofan_zhou@scau.edu.cn (XZ), wjh0505@gmail.com (JW) and zls83@zju.edu.cn (LZ))
†These authors contributed equally to this study.

Keywords: *Eustoma grandiflorum*, genome assembly, whole-genome triplication event, flower coloration, floral development model.

Introduction

Eustoma grandiflorum (lisianthus) is a Gentianaceae-family ornamental plant. Because of its enormous rose-like blossoms, long stems and extended vase life, its sales have increased dramatically in recent years, earning it the title of 'next rose'. Selective breeding has produced commercial lisianthus with a wide range of flower colours and shapes (Figure S1a; Li et al., 2022). In polyploid crops including wheat, cotton, peanuts and others, polyploidy is critical for the development of high-quality traits (Cheng et al., 2018). Polyploidy may also contribute to the development of desirable traits in cultivated lisianthus. Here, we report a high-quality chromosome-scale genome assembly for *E. grandiflorum* ($2n = 6x = 72$) using a combination of PacBio HiFi reads and Hi-C scaffolding technology and reveal that polyploidy domestication of lisianthus contributes to ornamental traits in cultivated lisianthus.

A total of 32.05 Gb (~23.56X) of PacBio HiFi data and 140.14 Gb (~103.04X) Hi-C data were generated for *de novo* whole-genome sequencing. The total length of the assembly was 1.71 Gb, comprising 1056 contigs with a corresponding N50 of 7.33 Mb (Table S1), and 36 pseudo-chromosomes were assembled (Figures S1 and S2, Table S2). BUSCO revealed a completeness rate of 94.7% and a duplication rate of 31.6% (Table S5). A total of 54 305 high-quality protein-coding genes were predicted (Tables S3–S8). In addition, 77.85% of the genome was annotated to be repeat sequences (Tables S9–S12).

Genome collinearity identified a large number of collinear blocks with a ratio of 6 : 1 between *E. grandiflorum* and *Gelsemium sempervirens* (Figure 1a), and a ratio of 2 : 1 between *E. grandiflorum* and *E. grandiflorum* (Figure S3), indicative of polyploidy events' existence. To this end, the 36 pseudo-chromosomes could be divided into three subgenomes, then 12 homologous groups with three sets of monoploid chromosomes: A, B and C were obtained according to the transposable element profiles (Figure S4, Table S10–S12). The reasonable collinearity within subgenomes suggested that *E. grandiflorum* had experienced a whole-genome duplication (WGD) event in the recent history of *E. grandiflorum* (Figure S5). The *Ks* distribution further confirmed that *E. grandiflorum* experienced a WGD event (*Ks* peak value = 0.93) and a whole-genome triplication (WGT) event (Ks peak value = 0.21) after divergence from *Calotropis gigantea*, which is consistent with the ratio of 6 : 1 (*E. grandiflorum*: *G. sempervirens*) and the evolutionary relationships depicted by the phylogenetic tree (Figures 1a, S6–S7).

A total of 15 436 genes belonging to syntenic gene groups resulting from the WGT event were found based on collinearity across *E. grandiflorum* subgenomes, which were enriched in processes of external stimulus response, anatomical structure morphogenesis and biosynthetic process (Figure S8, Table S13). Substantial copy number variations of transcriptional factors (TFs) and structural genes participating in flavonoid/anthocyanin biosynthesis were discovered as a result of WGT including *MYBs*, *bHLHs*, *CHIs*, *CHSs*, *DFRs*, *GTs* and *FLSs* (Figures S9–S15). Thus, it was hypothesized that the polyploidy event would enable the breeding of colourful lisianthus varieties by providing enhanced genetic materials for anthocyanin production. We also found that numerous TFs regulating organ/flower development were generated by WGT, including floral identity genes in the MADS family, and members in the TCP family and HD-Zip III family, which might influence the formation of *E. grandiflorum's* flower morphology (Figures 1d, S16–S17).

To examine the genetic pathways regulating flower pigmentation in lisianthus, we performed RNA-seq of petals in the purple lisianthus (Purple01), the green lisianthus (Green01), the yellow lisianthus (Yellow01), the red lisianthus (Red01) and 'Rosita White' at different stages (bud stage, S1; turning stage, S2; blooming stage, S3) and conducted weighted correlation

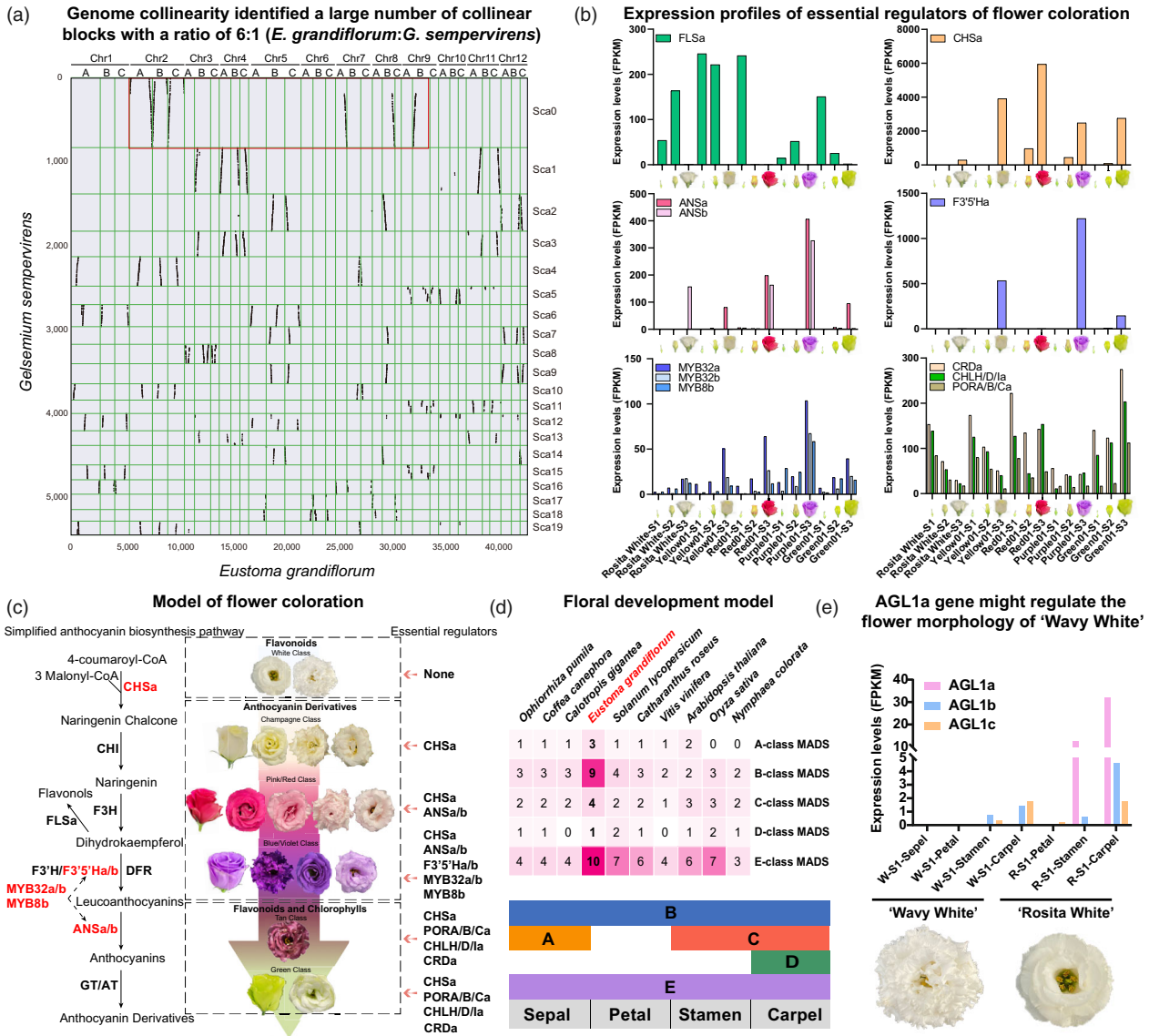

Figure 1 (a) Alignment of *Eustoma grandiflorum* chromosomes with *Gelsemium sempervirens* scaffolds. (b) Histograms showing expression profiles of essential regulators of flower coloration in lisianthus. S1, bud stage; S2, turning stage; S3, blooming stage. FLS, flavonol synthase; CHS, chalcone synthase; ANS, anthocyanidin synthase; F3′5′H, flavonoid 3′,5′-hydroxylase; CRD, Mg-protoporphyrin IX monomethyl ester cyclase; CHLH/D/I, Mg-chelatase subunits H, D and I; PORA/B/C, protochlorophyllide reductase. (c) A proposed model of flower coloration in lisianthus. The potential simplified anthocyanin biosynthesis pathway in lisianthus is depicted. CHI, chalcone isomerase; F3H, flavanone 3-hydroxylase; F3′H, flavonoid 3′-hydroxylase; DFR, dihydroflavonol-4-reductase; GT, glucosyltransferase; AT, acyltransferase. Essential regulators of flower coloration in lisianthus are in red fonts. The main pigments refer to the reference (Gao and Li, 2020). (d) A proposed floral development model of lisianthus based on the expression patterns of floral identity genes. Heatmap shows the number of MADS genes across various species. (e) Histograms showing the expression levels of C-class MADS genes in lisianthus. In all samples, *AGL1d* is zero in FPKM, hence it is not displayed.

network analysis (WGCNA) (Figure S18). Genes involved in flavonoid biosynthesis were identified, and the putative anthocyanin biosynthesis pathway was depicted (Figures 1c, S11–S15, S19). We found that *FLSa* was highly expressed in S1 and S2, and was barely expressed in S3 (Figure 1b). In S3, we found that *CHSa* expression level was significantly higher in all coloured cultivars than in white cultivars, and *ANSa/b* displayed much higher expression levels in both pink/red and blue/violet cultivars (Figures 1b, S20). Moreover, compared to pink/red lisianthus, blue/violet lisianthus showed higher *F3′5′Ha/b* levels (Figures 1b, S20). Co-expression network reconstruction of the module specific to S3 of lisianthus Purple01 ('darkorange2' module in Figure S18) identified several *MYBs* co-expressed with *F3′5′Ha* and *ANSa/b*; among them, *MYB32a*, *MYB32b* and *MYB8b* showed high expression levels in S3 of lisianthus Purple01 similar to those of *F3′5′Ha* and *ANSa/b* during flower development (Figures 1b, S21). As a result, we suggested that in lisianthus *CHSa*, *ANSa/b*, *F3′5′Ha/b*, *MYB32a/b* and *MYB8b* codetermine blue/violet flower coloration, *CHSa* and *ANSa/b* codetermine pink/red flower coloration and *CHSa* determines yellow flower coloration (Figure 1c).

Instead of accumulating anthocyanins in the blooming stage, green lisianthus varieties synthesize and accumulate large amounts of chlorophylls, leading to green phenotypes. *CHLMa*,

CRDa and *PORA/B/Ca* were assumed to be important regulators of chlorophyll biosynthesis in petals since they had the highest expression levels in S3 in lisianthus Green01 (Figure 1b). Multiple genes involved in photosynthesis, including those encoding Chlorophyll a/b-binding proteins (CABs), were found to be co-expressed with *CHLMa*, *CRDa* and *PORA/B/Ca*, suggesting that these CABs might also play important roles in green petal formation by inhibiting chlorophyll degradation via forming antenna complexes with free chlorophylls (Figures S22–S24). Based on the same expression patterns of genes involved in chlorophyll synthesis and photosynthesis (e.g. *CABs*) in the tan lisianthus with those in lisianthus Green01, it is possible that chlorophylls were also pigments in the tan lisianthus (Figures 1c, S24–S25).

In lisianthus, a total of 120 MADS-box genes were identified, including 27 floral organ identity genes (three A-class genes, nine B-class genes, four C-class genes, one D-class genes and 10 E-class genes; Figures 1d, S26–S28). The floral development model in *E. grandiflorum* was constructed according to floral identity genes' expression profiles (Figures 1d, S30). We found that multiple floral organ identity genes were generated by WGT, including B-class *AP3s*, C-class *AGL1s* and E-class *AGL9s*, which might influence the evolution of *E. grandiflorum*'s flower morphology (Li et al., 2022; Figure S29). 'Rosita White' and 'Wavy White' are two popular lisianthus cultivars, which have flat-shaped petals and wave-shaped petals respectively. We found that *AGL1a*, a C-class MADS gene, was highly expressed in the stamen and carpel of 'Rosita White', while it was barely expressed in all the flower tissues of 'Wavy White', potentially due to differences in cis-acting regulatory elements between their promoters (Figures 1e, S30–S31). It was reported that the absence of C-class *MADSs* could result in the double-flower phenotype. Thus, we speculated that *AGL1a* could be linked to the more apparent double-flower phenotype with more petal numbers of 'Wavy White' (Figure S32).

In summary, we present the chromosome-level genome of *E. grandiflorum* and identify the key candidate genes involved in flower coloration and morphology, which will speed up the molecular breeding of *E. grandiflorum* in the future.

Acknowledgements

We thank Yunnan Fundamental Research Projects (202201AU070168) for funding resources, and the High-level Talent Introduction Program of Yunnan Province-Industrial Talent Special Project (YNQR-CYRC-2020-004).

Conflict of interest

The authors declare no conflicts of interest.

Authors' contributions

Y. L. analysed the data and wrote the manuscript. F. L., J.W. and L. Z. conceived the study. Other authors carried out analysis and experiments.

Data availability statement

All data are publicly available in the BIG Data Center (https://bigd.big.ac.cn/) under project number PRJCA010064. And the genome assembly sequences and gene annotations are available at https://figshare.com/s/5e570b76c63f159b8da1.

References

Cheng, F., Wu, J., Cai, X., Liang, J., Freeling, M. and Wang, X. (2018) Gene retention, fractionation and subgenome differences in polyploid plants. *Nat. Plants* **4**, 258–268.

Li, F., Cheng, Y., Yu, R. and Yang, C. (2022) Genome Size and Ploidy Level of Commercial *Eustoma grandiflorum* (Raf.) Shinners. *J. Agric. Sci. Technol.* **24**, 739–748.

Gao, S. and Li, T.L. (2020) Relationship between the composition of Anthocyanins and flower color variation in Lisianthus (*Eustoma grandiflorum*). *J. Shenyang Agric. Univ.* **4**, 410–416 [in Chinese].

Supporting information

Additional supporting information may be found online in the Supporting Information section at the end of the article.

Figure S1-S32 Supplementary Figures.
Table S1-S14 Supplementary Datasets.
Appendix S1 Plant materials.

